



# Preparation and properties of Al-PILC supported $\text{SO}_4^{2-}/\text{TiO}_2$ superacid catalyst

Yue-Xiu Jiang, Xiao-Mei Chen, Yun-Fen Mo, Zhang-Fa Tong\*

*School of Chemistry and Chemical Engineering, Guangxi University, Nanning 530004, PR China*

Received 6 July 2003; received in revised form 6 December 2003; accepted 12 December 2003

## Abstract

$\text{SO}_4^{2-}/\text{TiO}_2/\text{Al}$ -pillared clay (ST/Al-PILC) superacid catalyst was prepared by loading active component  $\text{SO}_4^{2-}/\text{TiO}_2$  on Al-pillared clay. The texture structure properties of the catalyst were studied by means of X-ray powder diffraction and the adsorption of  $\text{N}_2$ . Acidity properties of the catalyst were tested by Hammett indicator method and FT-IR spectra of adsorbed pyridine technique. The characterization results indicated that Al-PILC carrier could inhibit the formation of anatase  $\text{TiO}_2$  and the transformation of anatase  $\text{TiO}_2$  into rutile  $\text{TiO}_2$ . ST/Al-PILC catalyst possesses both Lewis and Brønsted acid sites, and the number of acid sites on ST/Al-PILC is much larger than that on Al-PILC carrier, but its acid strength is lower than that of ST. Experimental results show that ST/Al-PILC is an effective catalyst for esterification of *n*-pentanol with benzoic acid.

© 2004 Elsevier B.V. All rights reserved.

**Keywords:** Solid superacid; Sulfated titania; Al-pillared clay; Catalyst; Characterization

## 1. Introduction

Pillared clays, a peculiar type of porous and high surface area solid material, have attracted considerable attention for application as catalysts, catalytic supports, and sorbents. They are prepared by intercalating polycations into the interlayer region of expandable clay materials. After calcination, the polycations were converted into robust metal oxide pillars, expanding the layers of the clay.

Pillared clays can be used for many acid-catalyzed reactions [1–3], but they are less efficient for those reactions need strong acidity catalyst, which limits their application. Some attempts at improving and controlling the acidity of pillared clays have been done such as changing the type of the host matrix [4], varying the identity of the pillar [5] and introducing sulfate ion to the pillared clays [6,7]. Hence, we have attempted to enhance the acidity by loading  $\text{SO}_4^{2-}/\text{TiO}_2$  on Al-pillared clay.

$\text{SO}_4^{2-}/\text{M}_x\text{O}_y$  solid superacid ( $\text{M}_x\text{O}_y$  are usually some transition metal oxides such as  $\text{ZrO}_2$ ,  $\text{TiO}_2$ ,  $\text{Fe}_2\text{O}_3$  and so on) is a new type of catalyst, it has some advantages such as its high acid strength, no corrosion for the reactor, and

free from pollution. So it has been extensively used in many organic catalytic reactions of esterification, isomerization of *n*-alkanes, polymerization, acylation and so on. However,  $\text{SO}_4^{2-}/\text{M}_x\text{O}_y$  also has some disadvantages such as hard to adjust its acidity and small in surface area. Recently, Liao et al. [8] and Lopez et al. [9] reported that it is helpful to add some new component to  $\text{SO}_4^{2-}/\text{M}_x\text{O}_y$ , and a more effective way is to support  $\text{SO}_4^{2-}/\text{M}_x\text{O}_y$  on the porous materials with high surface area [10–12].

In this paper, solid superacid catalyst (ST/Al-PILC) was prepared, its physical properties were studied by X-ray powder diffraction and the adsorption of  $\text{N}_2$ . Acidity properties of the catalyst were tested by Hammett indicator method and FT-IR spectra technique. Catalytic activity of the catalyst was investigated by the esterification of pentanol with benzoic acid.

## 2. Experimental

### 2.1. Materials

Bentonite was obtained from Ningmin County, Guangxi Zhuang Autonomous Region and its chemical composition is given in Table 1. Other reagents used in this work were all A.R.

\* Corresponding author. Tel.: +86-771-3233728; fax: +86-771-3233718.

E-mail address: [bioche@gxu.edu.cn](mailto:bioche@gxu.edu.cn) (Z.-F. Tong).

Table 1  
The chemical composition of Ningming bentonite

Composition	Content (%)
SiO <sub>2</sub>	64.53
Al <sub>2</sub> O <sub>3</sub>	17.86
TiO <sub>2</sub>	0.38
Fe <sub>2</sub> O <sub>3</sub>	3.23
CaO	1.69
MgO	3.05
K <sub>2</sub> O	1.17
Na <sub>2</sub> O	1.27

## 2.2. Preparation of ST/Al-PILC

### 2.2.1. Preparation of Al-PILC

Ningming bentonite was purified by use of the sedimentation technique and converted to Na-bentonite by ion exchange reaction. Al-pillared clay was prepared by microwave irradiation method [13]. The Al-polyoxocation pillaring solution was prepared by drop-wise addition of 0.25 M NaOH to 0.2 M AlCl<sub>3</sub> under vigorous stirring, with a molar ratio OH<sup>-</sup>/Al<sup>3+</sup> = 2 and treated with microwave radiation for 10 min. A concentration of 10% (by mass) clay suspension was prepared by adding Na-bentonite to the distilled water. Then Al-polyoxocation solution was slowly added to the clay suspension and stirred for 3 h at 353 K. The ratio of Al/clay was 5 mmol of aluminum per gram of clay. The Al-pillared clay was separated by filtration and washed until chloride free, then was dried in an oven at 383 K and calcined at 573 K.

### 2.2.2. Preparation of ST/Al-PILC

Al-PILC was impregnated with an aqueous solution containing the requisite quantities TiCl<sub>4</sub> for 1 h, then 28% (by mass) ammonia solution was added to the suspension until pH 8–9 under vigorous stirring. The solid was separated by filtration and washed until chloride free, dried at 383 K and ground to 100–120 mesh. The powder was impregnated with a certain concentration of (NH<sub>4</sub>)<sub>2</sub>SO<sub>4</sub> solution for 8 h, followed by filtration, drying, and calcination in air at different temperatures for 3 h.

### 2.2.3. Preparation of ST

TiCl<sub>4</sub> was gradually added to distilled water, then 28% (by mass) ammonia solution was added until pH 8–9 under vigorous stirring. The solid in the solution was separated by filtration and washed until chloride free, dried at 383 K and ground to 100–120 mesh. The powder was impregnated with 1.0 M (NH<sub>4</sub>)<sub>2</sub>SO<sub>4</sub> solution for 8 h, followed by filtration, drying, and calcination at 773 K for 3 h.

## 2.3. Sample characterization

X-ray powder patterns had been recorded on a Rigaku D/MAX 2500 V diffractometer, with a copper tube as radiation source ( $\lambda = 1.54178 \text{ \AA}$ ) and operating at 40 kV

and 120 mA, its profiles were recorded at 2° (2 $\theta$ ) per minute.

The pore structures of samples were characterized on a Micromeritics ASAP2010 gas adsorption analyzer by N<sub>2</sub> adsorption–desorption isotherms at liquid N<sub>2</sub> temperature. Before measurements, the samples were degassed at 473 K for 2 h under vacuum. The average pore diameter was calculated using the BJH method based on the desorption isotherm, and surface area was calculated by using the BET method adsorption isotherm.

The maximum acid strength of samples characterized by a Hammett indicator method. The sample was pretreated by being evacuated at 423 K for 30 min, then cooled to room temperature and contacted to the vapor of the Hammett indicator. The acidic strength was determined by observing the color change of the indicator adsorbed on the surface of the sample. The indicators used in this work were *p*-nitrofluorobenzene ( $H_0 = -12.44$ ) and 2,4-dinitrotoluene ( $H_0 = -13.75$ ), the solvent used was *n*-heptane.

FT-IR spectra of chemisorbed pyridine on the sample were obtained by using a Spectrum 2000 FT-IR spectrometer. The samples were pressed into self-supporting wafers. The wafers were mounted in an infrared vacuum cell and degassed at 523 K for 2 h under vacuum ( $1 \times 10^{-2}$  Pa). Then cooled to 383 K and exposed to pyridine vapor for 15 min, desorption was performed by evacuation at 523 K.

The sulfur content in the catalysts was detected by using a chemical method. Dehydrated Na<sub>2</sub>CO<sub>3</sub> and ZnO were used as fusing agents, and the sulfate was turned into BaSO<sub>4</sub> and determined by a gravimetric method.

## 2.4. Catalytic testing

The esterification of *n*-pentanol with benzoic acid was used as a model reaction to test for the catalytic activity. The reaction was performed at atmospheric pressure and refluxing temperature in three-neck flask equipment with condenser and water separator, heated by a controlled electrical oven. The molar ratio of benzoic acid:*n*-pentanol was 1:3, the weight of a catalyst used was 8 wt.% of benzoic acid. When the reactant system was heated to the reaction temperature, the catalyst was added into the system. The conversion of benzoic acid was measured by the final and initial acid value of the reaction mixture.

## 3. Results and discussion

### 3.1. The acid strength of catalyst

The acid strengths of the samples determined with the Hammett indicators are listed in Table 2. From the table it can be seen that all ST/Al-PILC catalysts show lower acid strength than ST, although some of them also have superacidity. The acid strength decreases with the decrease in the loading of TiO<sub>2</sub>. When the loading of TiO<sub>2</sub> is less than 29.5 wt.%, the samples have no superacidity. In the following

Table 2  
Acid strengths of various samples

Samples	<i>p</i> -Nitrofluorobenzene	2,4-Dinitrotoluene
ST	+	+
20.5% ST/Al-PILC	–	–
25% ST/Al-PILC	±	–
29.5% ST/Al-PILC	+	±

*p*-Nitrofluorobenzene:  $H_0 = -12.44$ ; 2,4-dinitrotoluene:  $H_0 = -13.75$ ; (+) color changes clearly; (–) color does not change; (±) color changes unclearly.

work, 29.5 wt.% was chosen as the loading of  $TiO_2$  on the Al-PILC.

### 3.2. The Lewis and Brönsted acidity of catalyst

FT-IR spectra of chemisorbed pyridine (Py-IR) were used to distinguish the Lewis and Brönsted acid sites on the sample. Fig. 1 displays the Py-IR spectra of ST/Al-PILC and Al-PILC. In the region  $1400\text{--}1700\text{ cm}^{-1}$ , three peaks due to C–C stretching vibrations of pyridine are observed. The peak at  $1447\text{--}1449\text{ cm}^{-1}$  was assigned to pyridine adsorbed on Lewis acid sites, the peak at  $1544\text{--}1545\text{ cm}^{-1}$  is characteristic of pyridine adsorbed on Brönsted, while the peak at  $1490\text{ cm}^{-1}$  appears commonly for pyridine adsorbed on both Brönsted and Lewis acid sites. From the Py-IR spectra we can see that the number of acid sites on ST/Al-PILC is much larger than that on Al-PILC carrier.

### 3.3. The texture structure of catalyst

The X-ray powder diffraction patterns of samples calcined at different temperatures for 3 h are shown in Fig. 2. The results revealed that  $TiO_2$  is in an amorphous state when the sample was calcined at 573 K, the formation of anatase  $TiO_2$  started beyond 673 K, all the diffraction peaks ( $2\theta = 25.3^\circ, 37.9^\circ, 48.0^\circ, 55.0^\circ$ ) of anatase  $TiO_2$  appeared when calcination temperature is up to 773 K, and no lines due to rutile  $TiO_2$  were observed even when the calcination temperature is as high as up to 973 K. According to literature [14], for  $SO_4^{2-}/TiO_2$  superacid, the formation of anatase  $TiO_2$  starts beyond 573 K, and some apparent diffraction peaks of rutile  $TiO_2$  were observed after calcination at 948 K. Hence, it can be proposed that Al-PILC carrier inhibited the forma-

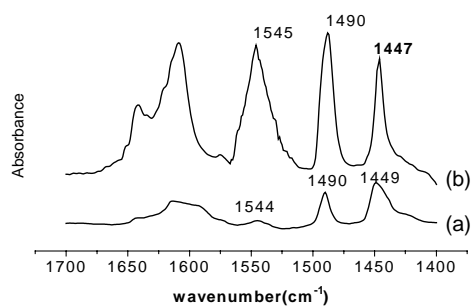


Fig. 1. Py-IR spectra of samples: (a) Al-PILC; (b) ST/Al-PILC.

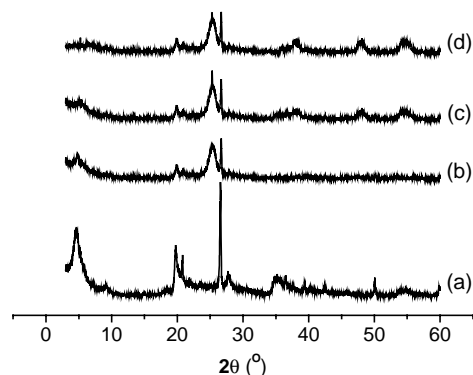


Fig. 2. XRD patterns of ST/Al-PILC calcined at different temperatures: (a) 573 K; (b) 673 K; (c) 773 K; (d) 973 K.

tion of anatase  $TiO_2$  and the phase transition from anatase to rutile crystalline form.

The X-ray patterns of samples also indicated that the support Al-PILC has interacted with ST when calcined at higher temperatures, because some diffraction peaks of Al-PILC disappeared or changed.

### 3.4. The surface area and the average pore diameter

The average pore diameter and the BET surface area of samples are given in Table 3. As can be noted from this table, there is a decrease in the average pore diameter and surface area of the sample after loading. This may be partly due to some of the  $TiO_2$  particles entering into the pores of Al-PILC and partially plugging the pores.

### 3.5. The sulfur content of the catalysts

Fig. 3 depicts the effect of  $(NH_4)_2SO_4$  solution concentration on the  $SO_4^{2-}$  loading of the samples. From Fig. 3 it can be seen that the  $SO_4^{2-}$  loading increased linearly with the  $(NH_4)_2SO_4$  solution concentration when  $[(NH_4)_2SO_4] < 1.0\text{ M}$  and changed insignificantly when  $[(NH_4)_2SO_4] > 1.0\text{ M}$ . This may be due to the  $SO_4^{2-}$  loading approached maximum as  $[(NH_4)_2SO_4] = 1.0\text{ M}$ .

### 3.6. The catalytic properties of catalyst

The effect of calcination temperature on the catalytic activity was shown in the Fig. 4. The results show that the catalytic activity of ST/Al-PILC calcined at 773–873 K is higher than that at other temperature, and climax appeared at 823 K. In the case of ST, when the thermal treating tem-

Table 3  
The surface area and the pore diameter of samples

Sample	$S_{BET}(\text{m}^2\text{ g}^{-1})$	Pore diameter ( $\times 10^{-9}\text{ m}$ )
Al-PILC	215	3.9
ST/Al-PILC	149	3.2

Calcination temperature: 773 K; calcination time: 3 h.

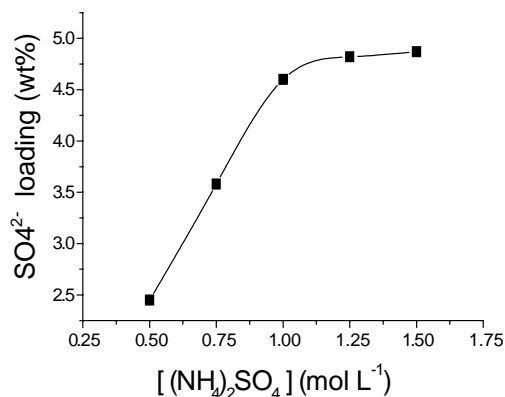


Fig. 3. Effect of [(NH<sub>4</sub>)<sub>2</sub>SO<sub>4</sub>] on the SO<sub>4</sub><sup>2-</sup> loading of the samples.

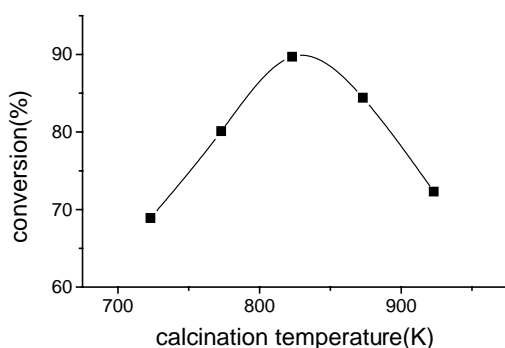


Fig. 4. Effect of calcination temperature on the conversion of benzoic acid. Benzoic acid:*n*-pentanol molar ratio = 1:3; reaction time = 3 h.

perature reaches over 823 K, its activity usually drops significantly because of the loss of sulfur absorbed on the surface. It is known that the generation of super acid sites in the system of SO<sub>4</sub><sup>2-</sup>/M<sub>x</sub>O<sub>y</sub> solid superacid is necessarily promoted by the sulfur of the metal oxides [15], the more acid sites formed, the higher catalytic activity exhibited. Therefore, it is reasonable to suggest that Al-PILC carrier can effectively retard the loss of sulfur during the calcination and enhance the thermal stability of catalyst.

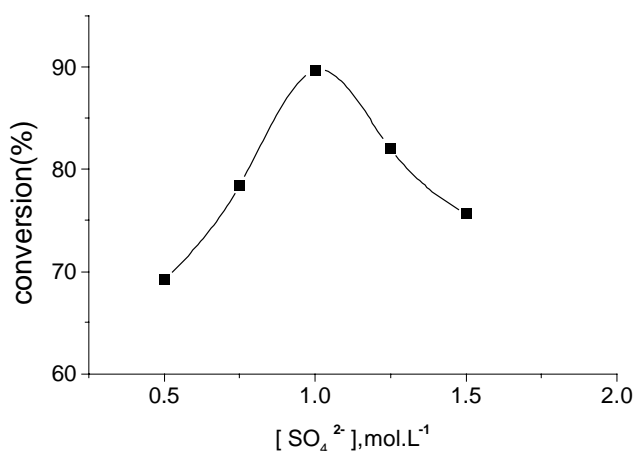


Fig. 5. Effect of [SO<sub>4</sub><sup>2-</sup>] on the conversion of benzoic acid. Benzoic acid:*n*-pentanol molar ratio = 1:3; reaction time: 3 h.

Fig. 5 shows the influences of the concentrations of the (NH<sub>4</sub>)<sub>2</sub>SO<sub>4</sub> impregnating solution on the catalytic activity of ST/Al-PILC (calcined at 823 K), the conversion of benzoic acid increases with the increase of the SO<sub>4</sub><sup>2-</sup> concentration in the low concentration range and reaches the maximum when [SO<sub>4</sub><sup>2-</sup>] = 1.0 M. After that it decreases with the increase of [SO<sub>4</sub><sup>2-</sup>]. This may be explained that it is unfavorable for forming sulfur complexes when SO<sub>4</sub><sup>2-</sup> concentration is low, and excessive SO<sub>4</sub><sup>2-</sup> on the catalyst surface forms inactive sulfate species, which cover the active sites.

#### 4. Conclusions

Al-PILC supported SO<sub>4</sub><sup>2-</sup>/TiO<sub>2</sub> (ST/Al-PILC) catalyst for esterification was prepared, and its acid strength is lower than that of ST. Py-IR spectra showed that ST/Al-PILC catalyst possesses both Lewis and Brønsted acid sites, and the number of acid sites on ST/Al-PILC is much larger than that on Al-PILC carrier. The X-ray patterns indicated that Al-PILC carrier can inhibit the formation of anatase TiO<sub>2</sub> and the transformation of anatase TiO<sub>2</sub> into rutile TiO<sub>2</sub>. ST/Al-PILC calcined at 823 K and impregnated with 1.0 M (NH<sub>4</sub>)<sub>2</sub>SO<sub>4</sub> solution exhibited the best catalytic activity for esterification of *n*-pentanol with benzoic acid.

#### Acknowledgements

We are grateful to the financial supports from The Key Laboratory of Science and Technology of Controllable Chemical Reactions BUCT, Ministry of Education, China, and the National Science Foundation of China (no. 29806004).

#### References

- [1] R. Mokaya, W. Jones, *J. Catal.* 153 (1995) 76.
- [2] M.J. Martínez-Ortiz, G. Fetter, J.M. Domínguez, J.A. Melo-Banda, R. Ramos-Gómez, *Microporous Mesoporous Mater.* 58 (2003) 73.
- [3] T. Cseri, S. Bekassy, F. Figueras, S. Rizner, *J. Mol. Catal.* 98 (1995) 101.
- [4] R. Molina, A. Schutz, G. Poncelet, *J. Catal.* 145 (1994) 79.
- [5] D. Tichit, F. Figueras (Eds.), *Pillared Layer Structures: Current Trends and Applications*, vol. 1, Elsevier, Amsterdam, 1990, p. 149.
- [6] H.L. Del Castillo, A. Gil, P. Grange, *Catal. Lett.* 43 (1997) 133.
- [7] L.K. Boudali, A. Ghorbel, D. Tichit, B. Chiche, R. Dutartre, F. Figueras, *Microporous Mater.* 2 (1994) 525.
- [8] S.J. Liao, Z.X. Yang, W.W. Yu, J.H. Hu, L.F. Wang, Z.T. Huang, *J. Mol. Catal.* 12 (1998) 292 (in Chinese).
- [9] T. Lopez, J. Navarrete, R. Gomez, O. Novaro, F. Figueras, H. Armandariz, *Appl. Catal. A: Gen.* 125 (1995) 217.
- [10] Y.Y. Huang, B.Y. Zhao, Y.C. Xie, *Chin. J. Catal.* 11 (1997) 493 (in Chinese).
- [11] T. Lei, W.M. Hua, Y. Tang, Y.H. Yue, Z. Gao, *Chem. J. Chin. Univ.* 21 (2000) 1240.
- [12] T. Lei, J.S. Xu, Y. Tang, W.M. Hua, Z. Gao, *Appl. Catal. A: Gen.* 192 (2000) 181.
- [13] A.M. de Andrés, J. Merino, J.C. Galván, E. Ruiz-Hitzky, *Mater. Res. Bull.* 34 (1999) 641.
- [14] Z. Gao, J.M. Chen, *Chem. J. Chin. Univ.* 15 (1994) 873.
- [15] T. Yamaguchi, *Appl. Catal. A: Gen.* 61 (1990) 1.